

# First principles viscosity and derived models for MgO-SiO<sub>2</sub> melt system at high temperature

Bijaya B. Karki,<sup>1,2,3</sup> Jian Zhang,<sup>1</sup> and Lars Stixrude<sup>4</sup>

Received 25 October 2012; revised 12 December 2012; accepted 13 December 2012; published 16 January 2013.

[1] The viscosity of silicate liquids at high temperature is crucial to our understanding of chemical and thermal evolution of the Earth since its early stages. First-principles molecular dynamics simulations of seven liquids across the MgO-SiO<sub>2</sub> binary show that the viscosity varies by several orders of magnitudes with temperature and composition. Our results follow a compensation law: on heating, the viscosity of all compositions approaches a uniform value at 5000 K, above which pure silica becomes the least viscous liquid. Viscosity depends strongly on composition (fourth power), implying a strong nonlinear dependence of the configurational entropy on composition. Using the simulation results, we derive and evaluate different types (Arrhenius and non-Arrhenius) of models for accurate description of the viscosity-temperature-composition relationship. Our results span the thermal regime expected in a magma ocean, and indicate that melt migration is important for understanding the generation and preservation of melts from frictional heating at very fast slip in impact processes. **Citation:** Karki B. B., J. Zhang, and L. Stixrude (2013), First principles viscosity and derived models for MgO-SiO<sub>2</sub> melt system at high temperature, *Geophys. Res. Lett.*, 40, 94–99, doi:10.1029/2012GL054372.

## 1. Introduction

[2] Viscous flow of silicate liquids is one of the primary agents of chemical and thermal evolution of the Earth [Miller *et al.*, 1991]. However, the viscosity over most of the relevant range of pressure, temperature, and composition remains unknown. While previous experimental studies have focused on conditions most relevant to shallow magma migration and volcanic eruption (temperature  $T < 1800$  K) [Giordano *et al.*, 2008], viscous flow of silicate melts is important for understanding their occurrence at much more extreme conditions, including atop the transition zone and the core-mantle boundary ( $T = 4000$  K) [Williams and Garnero, 1996; Song, 2004; Lee *et al.*, 2010]. Melting may have been

much more widespread in the past, possibly encompassing the entire mantle in a magma ocean with temperature exceeding 10,000 K [Reufer *et al.*, 2012]. Impacts may transiently generate even higher temperature melts, the viscosity of which is important for understanding melt generation and dispersal [Spray, 2010].

[3] First principles molecular dynamics simulations (FPMD) allow us to explore the viscosity of silicate liquids over a much wider range of temperature than have been accessed before. We can also explore a much greater compositional range than previous experiments, which have focused primarily on the range of natural lava compositions (rhyolite to basalt) [Shaw, 1972; Hui and Zhang, 2007; Giordano *et al.*, 2008]. Here, we report a first principles study of the melt viscosity of the entire MgO-SiO<sub>2</sub> binary system. The viscosity of anhydrous silicate melts is largely controlled by the degree of polymerization as measured by the ratio of non-bridging oxygens to tetrahedrally coordinated cations (NBO/T). While the vast majority of experimental data span a narrow range ( $0 < \text{NBO/T} < 1$ ), the MgO-SiO<sub>2</sub> join allows us to explore the entire range  $0 < \text{NBO/T} < \infty$ . The join consists of the two most abundant oxide components in Earth and encompasses ultra-mafic compositions that are more representative of the magma ocean and frictional melts [Spray, 1993]. Consisting of proto-typical network modifier (e.g., MgO, CaO, FeO) and network former (e.g., SiO<sub>2</sub>, Al<sub>2</sub>O<sub>3</sub>, TiO<sub>2</sub>), the join we focus on serves as a model system for an even wider range of natural melt compositions.

## 2. Method

[4] Our first principles molecular dynamics simulations are based on density functional theory [Kresse and Furthmüller, 1996]. The viscosity was computed using the Green-Kubo relation

$$\eta = \frac{V}{3k_B T} \int_0^\infty \left\langle \sum_{i < j} \sigma_{ij}(t + t_0) \cdot \sigma_{ij}(t_0) \right\rangle dt \quad (1)$$

where the integrand is the shear-stress autocorrelation function,  $\sigma_{ij}$  ( $i$  and  $j = x, y, z$ ) is the stress tensor, which is computed directly at every time step of the simulation,  $V$  is volume,  $k_B$  is the Boltzmann constant,  $T$  is temperature,  $t$  is time, and  $t_0$  represents the time origin (Figure S1). The local density approximation and projector augmented wave method were used as implemented in VASP with a plane wave cutoff of 400 eV and Brillouin zone sampling at the  $\Gamma$  point. Simulations consisted of 72–228 atoms. Simulation durations range from 30 ps to 1 ns with time step of 1 fs (silica liquid at 2750 K simulated for 3 ns with a time step of 3 fs). We examine seven compositions on the MgO-SiO<sub>2</sub> join (MgO, Mg<sub>5</sub>SiO<sub>7</sub>, Mg<sub>2</sub>SiO<sub>4</sub>, MgSiO<sub>3</sub>, MgSi<sub>2</sub>O<sub>5</sub>, MgSi<sub>5</sub>O<sub>11</sub>, and

All Supporting Information may be found in the online version of this article.

<sup>1</sup>Computer Science and Engineering Division, Louisiana State University, Baton Rouge, Louisiana, USA.

<sup>2</sup>Department of Geology and Geophysics, Louisiana State University, Baton Rouge, Louisiana, USA.

<sup>3</sup>Center for Computation and Technology, Louisiana State University, Baton Rouge, Louisiana, USA.

<sup>4</sup>Department of Earth Sciences, University College London, London, UK.

Corresponding author: B. B. Karki, Computer Science and Engineering Division, Louisiana State University, Baton Rouge, LA 70803, USA. (karki@csc.lsu.edu)

SiO<sub>2</sub>) at several temperatures from 2000–8000 K. We maintain the pressure at zero ( $\pm 1$  GPa) by adjusting the volume of the simulation cell at each temperature (Figure S2). Doubling the supercell size for selected compositions (MgO and MgSi<sub>5</sub>O<sub>11</sub>, each at 3000 and 6000 K) shows that the finite size effects are within statistical uncertainty. Further details of the computations can be found in our previous studies [Karki and Stixrude, 2010a; 2010b; Ghosh and Karki, 2011].

### 3. Viscosity Results and Models

[5] The shear stress auto-correlation function shows features characteristic of silicate liquids (Figure 1). An intermediate peak (near 0.05 ps) interrupts the monotonic decay of the autocorrelation function found in simple liquids [Levesque *et al.*, 1973]. This peak can be associated with the so-called cage effect seen also in self-diffusion of silicate liquids [Horbach and Kob, 1999]: on time scales intermediate to those of vibration and diffusion, atoms become temporarily trapped in cages of surrounding atoms from which they escape only after sufficient time. The intermediate peak in the stress auto-correlation function diminishes systematically in intensity with decreasing silica content and is absent for MgO, which behaves like a simple liquid. Moreover, the intermediate peak is substantially reduced in silica at higher temperature. Such a dynamical transition with increasing temperature or change in composition supports the basis of mode-coupling theory, which has found application in understanding the glass transition in a wide variety of systems [Horbach and Kob, 1999]. Our results indicate that mode-coupling theory is applicable to silicate liquids as well.

[6] The viscosity decreases monotonically on heating for all compositions, while the rate of change (i.e., the apparent activation energy  $E_A = R d \ln \eta / d(1/T)$ ) varies considerably with composition (Figure 2). The change of viscosity with temperature is largest for silica liquid with more than five orders of magnitude decrease from 2750 to 8000 K whereas it is smallest in MgO liquid—one order of magnitude over a similar temperature range. At low temperature, viscosity increases with silica content by five orders of magnitude

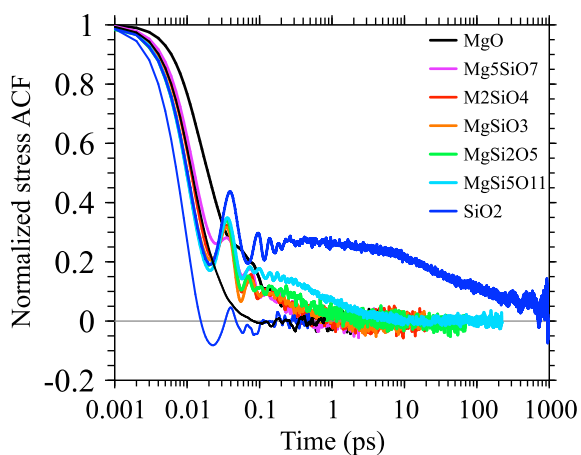


**Figure 1.** The calculated shear stress autocorrelation function (normalized ACFs) versus time at 3000 K for seven liquids as shown (thick lines), and at 6000 K for only end members (thin lines). The initial values of ACF are in the range of 2–5 GPa<sup>2</sup>.

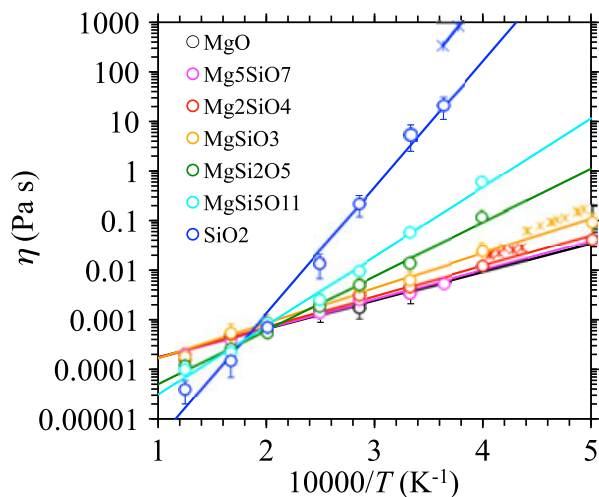


**Figure 2.** The FPMD viscosity results (circles) as a function of temperature (between 2000 and 8000 K) for seven liquids. Also shown are the experimental data (asterisks) for silica, enstatite, and forsterite liquids [Urbain *et al.*, 1982]. Lines are the Arrhenius fits ( $\ln \eta = A + E_A/(RT)$ ) independently performed for different liquids. Error bars are shown only for the end members and mid composition for the sake of clarity.

over the full compositional range at 2500 K. The FPMD results are in excellent agreement with experimental measurements [Urbain *et al.*, 1982] on MgSiO<sub>3</sub> and Mg<sub>2</sub>SiO<sub>4</sub> (differences of  $\sim 10\%$ ). The disagreement is larger in the case of the silica end-member (factor of 10), consistent with a previous pair potentials simulation study [Horbach and Kob, 1999], which may be attributed to dynamical transitions in silica liquid occurring at temperatures similar to that of our lowest temperature simulation [Kushima *et al.*, 2009], see Figure S3.

[7] The much more rapid decrease of viscosity on heating at the silica-rich end as compared with the MgO-rich end means that viscosities eventually cross: at high temperature, silica-rich liquids are less viscous (Figure 3a). The viscosity is independent of composition to within our uncertainty at an isoviscous temperature  $T_{\text{iso}} \sim 5000$  K. The crossover originates in a compensation law: a negative (linear) relationship between  $E_A$  and the viscosity at infinite temperature  $\ln \eta_{\infty}$  for different liquid compositions (Figure 3b). Via the Eyring relationship, we can relate this compensation law to that found for diffusion in a wide variety of systems: a positive linear relationship between the logarithm of diffusivity at infinite temperature and the activation energy. The compensation law for diffusion is associated with the isokinetic effect: for example, experimental data on silicate (solid) minerals show that Si, Mg-, and O self-diffusion coefficients converge around 2000 K [e.g., Winchell, 1969; Bejina and Jaoul, 1997; Zhao and Zheng, 2007].

[8] Our results do not support the notion of a universal high temperature limit to which the viscosity of all fluids smoothly converges [e.g., Giordano *et al.*, 2008]. Indeed, viscosity continues to depend significantly on composition even at 8000 K (Figure 2). The computed value of  $\ln \eta_{\infty}$  varies from  $-10$  to  $-18$  from the MgO to silica end (Figure 3b). The notion of a universal high temperature limit to viscosity is

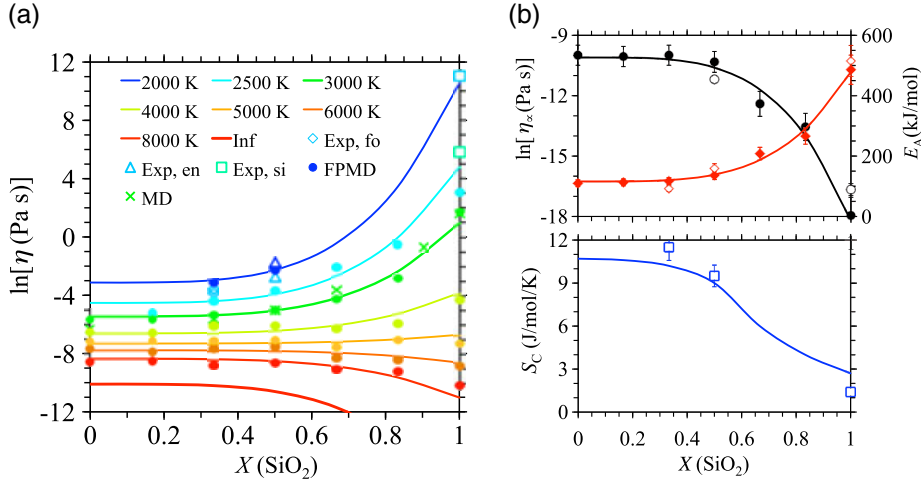


**Figure 3.** (a) Viscosity-composition isotherms (lines) computed with the global Arrhenius model (equation (2)) in comparison with the present FPMD (solid circles) and previous MD 3000 K results [crosses, *Lacks et al.*, 2007]. The molar fraction  $X$  of silica component takes values of 0, 1/6, 1/3, 1/2, 2/3, 5/6, and 1, respectively, for seven liquids  $\text{MgO}$ ,  $\text{Mg}_5\text{SiO}_7$ ,  $\text{Mg}_2\text{SiO}_4$ ,  $\text{MgSiO}_3$ ,  $\text{MgSi}_2\text{O}_5$ ,  $\text{MgSi}_5\text{O}_{11}$ , and  $\text{SiO}_2$  studied. The curves from the top to the bottom correspond to temperatures from 2000 K to infinite as shown. Open symbols are the experimental data for  $\text{Mg}_2\text{SiO}_4$ ,  $\text{MgSiO}_3$ , and  $\text{SiO}_2$  liquids in the temperature intervals of 2293–2461, 1987–2268, 2049–2755 K, respectively [*Urbain et al.*, 1982]. (b) The Arrhenius parameters:  $\ln \eta_\infty$  (solid circles) and  $E_A$  (solid diamonds) as computed for individual compositions and from the global Arrhenius model (equation (2)) (lines), and the experimentally derived values (open symbols) from *Urbain et al.* [1982]. Also shown is the configurational entropy ( $S_C$ ) estimated from values of  $E_A$ , the Adams-Gibbs theory, and assuming a value of  $B_E = 150$  kJ/mol (line). Experimental values (open symbols) are computed from the model of *Stebbins et al.* [1984].

based on the extrapolation of the viscosity of a variety of liquids (organic, ionic, metallic) to  $1/T \rightarrow 0$ . However, the extrapolation is long as experimental data extend only down to  $T_g/T = 0.3$  in the best case, where  $T_g$  is the glass transition temperature. Some analyses of silicate liquid viscosity have found that a universal value of  $\ln \eta_\infty$  is consistent with experimental data [*Russell et al.*, 2003; *Giordano et al.*, 2008]. However, the experimental data do not require  $\ln \eta_\infty$  be invariant with composition as the data do not probe temperatures much about the liquidus. Indeed, other models fit to similar data sets and, making different assumptions, have found that  $\ln \eta_\infty$  varies from  $-14$  to  $-9$  for an Arrhenian model [*Shaw*, 1972] or from  $-21$  to  $-3$  for a non-Arrhenian model [*Hui and Zhang*, 2007]. Analyses based on kinetic rate theory suggest  $\ln \eta_\infty = -10.5$ , similar to our value for the MgO-rich end. However, the kinetic rate theory estimate relies on assumptions about the value of the attempt frequency, the infinite frequency shear modulus, and the activation entropy of liquids at very high temperature, which are unknown perhaps to within several orders of magnitude, and which may vary considerably with composition at high temperature [*Toplis*, 1998].

[9] We find the microscopic origin of the high temperature viscosity crossover and reversal in an analysis of the liquid structure (Figure 4 and Table S1). The viscosity of silica-rich liquids varies more rapidly with temperature because the structure changes more profoundly. Silica has the highest viscosity of any silicate liquid at low temperature because of its unique structure: a continuous random network of corner-sharing polyhedra that is nearly perfect. In our simulations  $\sim 96\%$  Si atoms are fourfold coordinated with O atoms of which  $>99\%$  form interpolyhedral bridges at 3000 K ( $\text{NBO}/T < 0.005$ ). As temperature increases, Si-O bonds are progressively broken so that the network is substantially ruptured at high temperature: at 8000 K,

$\text{NBO}/T \sim 2.5$ . The ruptured structure of silica liquid contains large void spaces, resembling very low-density structures formed at low temperature either by the application of tensile stress or by the aerogel process [*Kieffer and Angell*, 1988]. Our high temperature structure differs from that of aerogel in having a number of two and threefold coordinated Si. The creation of large void spaces contributes to the rapid decrease of viscosity on heating via the increase in free volume [*Macedo and Litovitz*, 1965]: the volume per atom of silica liquid is larger than that of MgO liquid at 8000 K. In contrast, viscosity depends much more weakly on temperature toward the MgO-rich end because network connectivity is limited even at low temperature, with large  $\text{NBO}/T$  at all temperatures. Moreover, the presence of network modifying cations in more MgO-rich compositions prevents the formation of large void spaces because of longer and weaker Mg-O bonds compared to Si-O bonds.

[10] The highest temperature (8000 K) studied here is likely to be super-critical, at least for silica-rich compositions. The critical point for silica is determined experimentally to be 5130 K, 0.13 GPa [*Kraus et al.*, 2012]. However, we found no clear evidence of a liquid to vapor transition in our simulations: even at the highest temperature (8000 K) studied, the internal pressure still changes when the volume is varied demonstrating significant interatomic interactions. We therefore interpret our highest temperature results as representing super-heated liquids. The super-heated liquid regime has been studied previously with MD simulations [*Angell et al.*, 1987].

[11] The viscosity is a strong function of composition, much stronger than what is typically assumed in empirical fits to viscosity data. For example, at 3000 K, the viscosity varies by less than an order of magnitude over the range  $0 < X < 0.6$ , and then changes by more than two orders of magnitude from  $0.6 < X < 1$ , where  $X$  is the mole fraction of silica

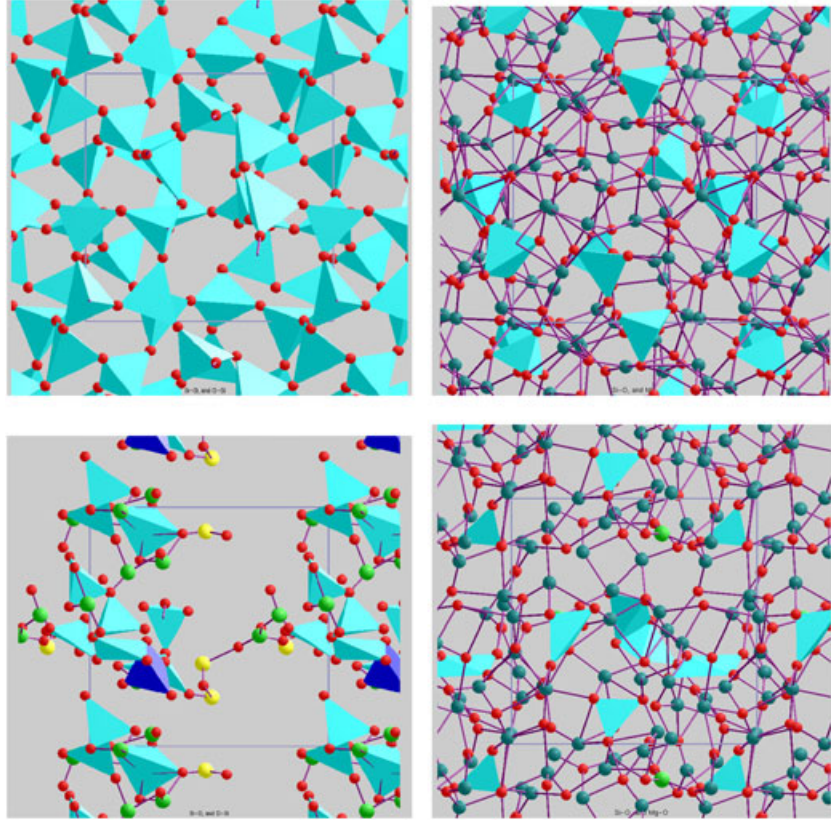


**Figure 4.** Visualization snapshots of simulated melt structures at 3000 K (top panel) and 6000 K (bottom panel) for SiO<sub>2</sub> (left) and Mg<sub>5</sub>SiO<sub>7</sub> (right) using visualization program of *Bhattacharai and Karki* [2009]. The Si-O coordination is comprised of tetrahedra (cyan), pentahedra (blue), twofold (yellow large sphere), and threefold (green large sphere) species in the left images. Small spheres (red) represent oxygen atoms whereas medium spheres (bluish green in right images) represent magnesium atoms.

(Figure 3). Similar behavior is also found in the Na<sub>2</sub>O-SiO<sub>2</sub> and H<sub>2</sub>O-SiO<sub>2</sub> systems, with the viscosity varying monotonically and much more rapidly at the silica rich end [*Toplis, 1998; Audetat and Keppler, 2004*]. While most experimentally based viscosity models [*Shaw, 1972; Hui and Zhang, 2007; Giordano et al., 2008*] assume a linear or quadratic dependence of the viscosity on  $X$ , we find that viscosity varies with the fourth power.

[12] The strong variation of viscosity with composition that we find lends important insight into the nature of the liquid structure along the join. The Adams-Gibbs theory relates the viscosity to the configurational entropy of the liquid  $\ln \eta = A + B_E / (TS_C)$ , where  $S_C$  is the configurational entropy and  $B_E$  is the energy term [*Adam and Gibbs, 1965*]. Along simple substitutional binaries, such as MgSiO<sub>3</sub>-CaSiO<sub>3</sub> [*Neuvill and Richet, 1991*], the variation of configurational entropy and viscosity with composition is symmetric; providing the motivation for linear and quadratic terms in the compositional dependence of the viscosity in many experimentally based viscosity models. For example, the viscosity shows a quadratic minimum on the MgO-SiO<sub>2</sub> join in a previous multi-component model [*Giordano et al., 2008*]. In contrast, the highly asymmetric and monotonic variation of viscosity with composition that we find shows that mixing on the MgO-SiO<sub>2</sub> join cannot be viewed as one of simple cation substitution, reflecting the very different coordinate environments of Si<sup>4+</sup> and Mg<sup>2+</sup>. The Arrhenian model entails a value of the ratio  $S_C/B_E$ , varying from

0.00017 to 0.00004 K<sup>-1</sup> from MgO to silica. The inferred entropy-composition trend is consistent with the experimental data (Figure 3b), which shows the configurational entropy decreases by a factor of 3 between MgSiO<sub>3</sub> and SiO<sub>2</sub> liquid at  $T/T_g = 1.5$ , where  $T_g$  is the glass transition temperature [*Stebbins et al., 1984*]. The higher configurational entropy for MgO-rich compositions arises because these liquids adopt a richer set (wider distribution) of Mg-O and Si-O coordination species and less stable Mg-O and Si-O bonds than silica-rich compositions do.

[13] We propose the following global model for the viscosity of the MgO-SiO<sub>2</sub> system

$$\ln \eta(T, X) = (A_0 + A_1 X^4) + \frac{E_{A0} + E_{A1} X^4}{RT} \quad (2)$$

which fits our results with a root mean square error (RMSE) of 0.34 ln units and uniform magnitudes of residuals over the entire range of viscosity considered (Figure S4). The optimized model parameters are given in Table 1 and the computed viscosity isotherms are shown in Figure 3a. Our results compare favorably with previous 3000 K results obtained from a force field calculations, which used larger and longer runs [*Lacks et al. 2007*]. It is worth noting that our model spans a much greater range of temperature (2000–8000 K) and composition (the entire possible range of NBO/T) compared to previous models [*Shaw, 1972; Hui and Zhang, 2007; Giordano et al., 2008*] and yet uses fewer parameters. The Arrhenian nature of the temperature dependence of

**Table 1.** The Optimized Coefficients and RMSE Values (Natural Log Units) for Four Models We Have Studied<sup>a</sup>

	Arrhenius (equation (2))	VFT (equation (3))	Equation (4)	Equation (5)
$A_0$	-10.1	-9.8	-9.4	-9.9
$A_1$	-8.1	-7.6	-6.5	-7.5
$E_{A0}$ or $B_0$	116	11,900	9300	11,700
$E_{A1}$ or $B_1$	362	38,900	21,400	38,300
$T_0$ or $\alpha$ or $C$		238	1.22	280
RMSE	0.34	0.33	0.31	0.33

<sup>a</sup> $A_0 \sim \ln \eta_\infty$  and  $A_1 \sim \ln \eta_\infty$  (where  $\eta_\infty$  in Pa s);  $E_{A0}$  and  $E_{A1}$  in kJ/mol,  $B_0$ ,  $B_1$ ,  $T_0$ , and  $C$  in K;  $\alpha$  is a dimensionless parameter.

viscosity in our simulations is remarkable in comparison with experimentally based models that tend to show much larger deviations from the Arrhenius behavior. We attribute this to the much lower temperatures typical of experiments on silicate liquids as compared with our results: deviations from Arrhenian behavior become most apparent as the temperature approaches the glass transition temperature. In order to further investigate possible deviations from Arrhenian behavior in our results, we consider three types of non-Arrhenian models [Mauro *et al.*, 2009], which were previously used for silicate liquids. First, the VFT (Vogel-Fulcher-Tamman) relation fit to the FPMD results is

$$\ln \eta(T, X) = (A_0 + A_1 X^4) + \frac{B_0 + B_1 X^4}{T - T_0} \quad (3)$$

[14] The value (-17.4) of  $\ln \eta_\infty$  for the silica end is comparable with the experiment-based value of -17.1 [Giordano *et al.*, 2006]. The parameter  $B$  increases with silica content more rapidly after the mid composition reaching 51,000 K for  $X=1$ . For comparison, the experimentally based value of  $B$  for silica is 63,000 K [Giordano *et al.*, 2006]. The fit to our results improves only marginally when a linear compositional dependence of  $T_0$  was assumed, and the VFT fit is not significantly better than the Arrhenian fit. The equation based on an atomic hopping approach is

$$\ln \eta(T, X) = (A_0 + A_1 X^4) + \left( \frac{B_0 + B_1 X^4}{T} \right)^\alpha \quad (4)$$

[15] Finally, the equation based on the temperature dependence of configurational entropy as required by the Adam-Gibbs relation is

$$\ln \eta(T, X) = (A_0 + A_1 X^4) + \left( \frac{B_0 + B_1 X^4}{T} \right) \exp\left(\frac{C}{T}\right) \quad (5)$$

[16] Table 1 shows the optimized values of coefficients and RMSE values for four models. The RMSE values and the level of fits for all our models are similar (Figure S4) and are comparable with those of previous multi-component viscosity models. For instance, multi-component non-Arrhenian model [Giordano *et al.*, 2008] has a RMSE of 0.9 ln units.

#### 4. Geophysical Implications

[17] Our FPMD results provide the first constraints on the viscosity of silicate liquids at low pressure and temperature exceeding 2800 K. Melts at temperatures far exceeding the

liquidus are produced during the contact and excavation stages of impacts [Spray, 2010]. For example, shockwave compression produced by a typical terrestrial impactor velocity yields a temperature of 5000 K on the liquid-vapor coexistence line after isentropic release [Kraus *et al.*, 2012]. Slip on shock veins and on faults during the excavation stage can generate even higher temperature. Impact melts once produced flow in response to deviatoric stresses. The rate of flow is governed by the viscosity and is important for understanding (i) the process of melt generation during slip on faults, which depends on a balance between the rate of slip, the rate of melt production, and the rate of melt escape from the slip zone and (ii) interpretation of geologic evidence for impact melts. As an example, consider the temperature rise due to frictional heating in fast slip  $\Delta T \sim \eta v^2/k \sim 10,000$  K for  $\eta = 10^{-3}$  Pa s (the isoviscous value, Figure 3), thermal conductivity  $k = 1$  W/m/K, and  $v = 3$  km/s, i.e., the shear wave velocity which is the upper limit for the slip rate. In the absence of melt escape, this degree of super-heating quickly causes the thickness of the melt zone to exceed the thermal diffusion length, and the rate of frictional heating to diminish [Melosh, 2005]. The importance of melt escape is measured by the ratio of the volumetric flow rate to the amount of melt remaining in the zone  $R \sim d^2 \tau / \eta v L \sim 100$  for  $d = 1$  mm, deviatoric stress  $\tau = 300$  MPa, and the fault length  $L = 1$  km [Melosh, 2005; Senft and Stewart, 2009]. The very low silicate melt viscosities that we find at high superheat makes flow important and means that melt zones may be maintained at high rates of frictional heating by keeping them thin. Melt flow and accumulation away from the slip zone may help to explain the very large thicknesses of frictional melt bodies in impact structures such as Sudbury impact structure [Melosh, 2005; Senft and Stewart, 2009].

[18] By combining our results with those of previous simulations [Karki and Stixrude, 2010a; 2010b; Ghosh and Karki, 2011], we estimate that the compensation law holds at elevated pressure as well as near ambient pressure, and that the isoviscous temperature,  $T_{\text{iso}}$  increases with increasing pressure. On the 6000 K isotherm, the viscosity of SiO<sub>2</sub> is less than that of MgSiO<sub>3</sub> at ambient pressure, but increases more rapidly with pressure so that they cross at 15 GPa, implying  $dT_{\text{iso}}/dP \sim 30$  K/GPa, and an isoviscous temperature at mid-mantle depth  $T_{\text{iso}} (P = 70 \text{ GPa}) \sim 7000$  K. The condition of isoviscosity is therefore relevant to conditions expected in the magma ocean. During the moon-forming impact, a substantial part of the mantle is heated to temperature exceeding 10,000 K [Reufer *et al.*, 2012], well above the isoviscous temperature. On cooling, the magma ocean passes through the isoviscous temperature, with the last super-liquidus isentrope varying from 2500 K at the surface to 4800 K at the base of the mantle [Stixrude *et al.*, 2009]. The proximity

of the magma ocean thermal regime to isoviscous conditions means that the dependence of viscosity on silicate composition in the magma ocean is much weaker or even opposite to the low temperature trend typified by lavas. This is significant because the viscosity of the super-liquidus magma ocean controls its cooling rate, and the rate of chemical differentiation via net vertical motion of silicate crystals or iron-rich blobs [Solomatov, 2007].

[19] **Acknowledgments.** This work was supported by the National Science Foundation grant (EAR-1118869) and the UK National Environmental Research Council grant (NE/ F01787/1). High-performance computing resources were provided by Louisiana State University (<http://www.hpc.lsu.edu>).

## References

- Adam, G., and J. H. Gibbs (1965), On the temperature dependence of cooperative relaxation properties in glass-forming liquids, *J. Chem. Phys.*, **43**, 139–146.
- Angell, C. A., P. A. Cheeseman, and R. G. Kadiyala (1987) Diffusivity and thermodynamic properties of diopside and jadeite melts by computer simulation studies, *Chem. Geol.*, **62**, 83–92.
- Audetat, A., and H. Keppler (2004), Viscosity of fluids in subduction zones, *Science*, **303**, 513–516.
- Bejina, F., and O. Jaoul (1997) Silicon diffusion in silicate minerals, *Earth Planet. Sci. Lett.*, **153**, 229–238.
- Bhattacharai, D., and B. B. Karki (2009), Atomistic visualization: Space-time multiresolution integration of data analysis and rendering, *J. Mol. Graph. Mod.*, **27**, 951–968.
- Ghosh, D. B., and B. B. Karki (2011), Diffusion and viscosity of Mg<sub>2</sub>SiO<sub>4</sub> liquid at high pressure from first principles simulations, *Geochim. Cosmochim. Acta*, **75**, 4591–4600.
- Giordano, D., et al. (2006), An expanded non-Arrhenian model for silicate melt viscosity: A treatment for metaluminous, peraluminous and peralkaline liquids, *Chem. Geol.*, **229**, 42–56.
- Giordano, D., J. K. Russell, D. B. Dingwell (2008), Viscosity of magmatic liquids: A model, *Earth Planet. Sci. Lett.*, **27**, 123–134.
- Horbach, J., and W. Kob (1999), Static and dynamic properties of viscous silica melt, *Phys. Rev. B*, **60**, 3169–3181.
- Hui, H., and Y. Zhang (2007), Toward a general viscosity equation for natural anhydrous and hydrous silicate melts, *Geochim. Cosmochim. Acta*, **71**, 403–416.
- Karki, B. B., and L. Stixrude (2010a), First-principles study of enhancement of transport properties of silica melt by water, *Phys. Rev. Lett.*, **104**, 215901.
- Karki, B. B., and L. Stixrude (2010b), Viscosity of MgSiO<sub>3</sub> liquid at Earth's mantle conditions: Implications for an early magma ocean, *Science*, **328**, 740–743.
- Kieffer, J., and C. A. Angell (1988), Generation of fractal structures by negative pressure rupturing of SiO<sub>2</sub> glass, *J. Non-Cryst. Solids*, **106**, 336–342.
- Kraus R. G. et al. (2012), Shock vaporization of silica and the thermodynamics of planetary impact events, *J. Geophys. Res.*, **117**, E09009.
- Kresse, G., and J. Furthmuller (1996), Efficiency of ab initio total energy calculations for metals and semiconductors using a plane-wave basis set, *Comput. Mat. Sci.*, **6**, 15–50.
- Kushima, A. et al. (2009), Computing the viscosity of supercooled liquids. II. Silica and strong-fragile crossover behavior, *J. Chem. Phys.*, **131**, 164505.
- Lacks, D. J., D. Rear, and J. A. Van Orman (2007), Molecular dynamics investigation of viscosity, chemical diffusivities and partial molar volumes along the MgO-SiO<sub>2</sub> join as functions of pressure, *Geochim. Cosmochim. Acta*, **71**, 1312–1323.
- Lee, C. A., et al. (2010), Upside-down differentiation and generation of a primordial lower mantle, *Nature*, **463**, 930–933.
- Levesque, D., L. Verlet, and J. Kurkijarvi (1973), Computer “experiments” on classical fluids. IV. Transport properties and time-correlation functions of the Lennard-Jones liquid near its triple point, *Phys. Rev. A*, **7**, 1690–1700.
- Macedo, P. B., and T. J. Litovitz (1965), On the relative roles of free volume and activation energy in the viscosity of liquids, *J. Chem. Phys.*, **42**, 245–256.
- Mauro, J. C., Y. Yue, A. J. Ellison, P. K. Gupta, and D. C. Allan (2009), Viscosity of glass-forming liquids, *Proc. Nat. Acad. Sci.*, **106**, 19780–19784.
- Melosh, H. J. (2005). in *Impact Studies*, C. Koeberl, H. Henkel (eds.). Impact Tectonics Book Series, Springer, Heidelberg, p. 55.
- Miller, G. H., E. M. Stolper, and T. J. Ahrens, (1991), The equation of state of a molten komatiite. 2. Application to komatiite petrogenesis and the hadean mantle, *J. Geophys. Res.*, **96**, 11849–11864.
- Neuville, D. R., and P. Richet (1991), Viscosity and mixing in molten (Ca, Mg) pyroxenes and garnets, *Geochim. Cosmochim. Acta*, **55**, 1011–1021.
- Reufer, A., M. Meier, W. Benz, and R. Wieler (2012), A hit-and-run giant impact scenario. *Earth Planet. Astrophys.*, <http://arxiv.org/pdf/1207.5224.pdf>
- Russell, J. K., D. Giordano, and D. B. Dingwell (2003), High-temperature limits on viscosity of non-Arrhenian silicate melts, *Am. Mineral.*, **88**, 1390–1394.
- Senft, L. E., and S. T. Stewart (2009), Dynamic fault weakening and the formation of large impact craters, *Earth Planet. Sci. Lett.*, **287**, 471–482.
- Shaw, H. R. (1972), Viscosities of magmatic silicate liquids: An empirical method of prediction, *Am. J. Sci.*, **272**, 870–893.
- Solomatov, V. S. (2007). in *Evolution of the Earth*, D. Stevenson, Ed., vol. 9 of *Treatise on Geophysics*, G. Schubert, Ed. Elsevier, Amsterdam, p. 91.
- Song, T. R., D. V. Helmberger, and S. P. Grand (2004), Low velocity zone atop the 410 seismic discontinuity in the northwestern United States, *Nature*, **427**, 530–533.
- Spray, J. G. (1993), Viscosity determinations of some frictionally generated silicate melts: Implications for fault zone rheology at high strain rates, *J. Geophys. Res. – Solid Earth*, **98**, 8053–8068.
- Spray, J. G., (2010), Frictional melting of planetary materials: From hypervelocity impact to earthquakes, *Ann. Rev. Earth Planet. Sci.*, **38**, 221–254.
- Stebbins, J. F., I. S. E. Carmichael, and L. K. Moret (1984), Heat capacities and entropies of silicate liquids and glasses, *Contrib. Mineral. Petrol.*, **86**, 131–148.
- Stixrude, L., N. de Koker, N. Sun, M. Mookherjee, and B. B. Karki (2009), Thermodynamics of silicate liquids in deep Earth, *Earth Planet. Sci. Lett.*, **278**, 226–232.
- Toplis, M. J. (1998), Energy barriers to viscous flow and the prediction of glass transition temperatures of molten silicates, *Am. Mineral.*, **83**, 480–490.
- Urbain, G., Y. Bottinga, and P. Richet (1982), Viscosity of liquid silica, silicates and aluminosilicates, *Geochim. Cosmochim. Acta*, **46**, 1061–1072.
- Williams, Q., and E. J. Garnero (1996), Seismic evidence for partial melting at the base of Earth's mantle, *Science*, **273**, 1528–1530.
- Winchell, P. (1969), The compensation law for diffusion in silicates, *High Temp. Sci.*, **1**, 200–215.
- Zhao, J. F., and Y. F. Zheng (2007), Diffusion compensation for argon, hydrogen, lead and strontium in minerals: Empirical relationships to crystal chemistry, *Am. Mineral.*, **92**, 289–308.